



ESTIMATING FLOODWATER DEPTHS FROM FLOOD INUNDATION MAPS AND TOPOGRAPHY¹

Sagy Cohen, G. Robert Brakenridge, Albert Kettner, Bradford Bates, Jonathan Nelson, Richard McDonald, Yu-Fen Huang, Dinuke Munasinghe, and Jiaqi Zhang²

ABSTRACT: Information on flood inundation extent is important for understanding societal exposure, water storage volumes, flood wave attenuation, future flood hazard, and other variables. A number of organizations now provide flood inundation maps based on satellite remote sensing. These data products can efficiently and accurately provide the areal extent of a flood event, but do not provide floodwater depth, an important attribute for first responders and damage assessment. Here we present a new methodology and a GIS-based tool, the Floodwater Depth Estimation Tool (FwDET), for estimating floodwater depth based solely on an inundation map and a digital elevation model (DEM). We compare the FwDET results against water depth maps derived from hydraulic simulation of two flood events, a large-scale event for which we use medium resolution input layer (10 m) and a small-scale event for which we use a high-resolution (LiDAR; 1 m) input. Further testing is performed for two inundation maps with a number of challenging features that include a narrow valley, a large reservoir, and an urban setting. The results show FwDET can accurately calculate floodwater depth for diverse flooding scenarios but also leads to considerable bias in locations where the inundation extent does not align well with the DEM. In these locations, manual adjustment or higher spatial resolution input is required.

(KEY TERMS: flood inundation; water depth; remote sensing; flooding.)

Cohen, Sagy, G. Robert Brakenridge, Albert Kettner, Bradford Bates, Jonathan Nelson, Richard McDonald, Yu-Fen Huang, Dinuke Munasinghe, and Jiaqi Zhang, 2017. Estimating Floodwater Depths from Flood Inundation Maps and Topography. *Journal of the American Water Resources Association* (JAWRA) 1-12. <https://doi.org/10.1111/1752-1688.12609>

INTRODUCTION

Over the years, a number of observational flood inundation mapping services have emerged. The Dartmouth Flood Observatory (DFO) (Accessed August 1, 2017, <http://floodobservatory.colorado.edu>)

and the Copernicus Emergency Management Service (Accessed August 1, 2017, <http://emergency.copernicus.eu>), for example, provide near-real-time inundation maps using satellite remote sensing. DFO provides daily global surface water maps based on 250-m spatial resolution Moderate Resolution Imaging Spectroradiometer (MODIS) imagery as well as higher

¹Paper No. JAWRA-17-0032-P of the *Journal of the American Water Resources Association* (JAWRA). Received March 26, 2017; accepted October 17, 2017. © 2017 American Water Resources Association. **Discussions are open until six months from issue publication.**

²Associate Professor (Cohen), Former Graduate Student (Bates), and Graduate Student (Munasinghe), Department of Geography, University of Alabama, Box 870322, Tuscaloosa, Alabama 35487; Professor (Brakenridge) and Research Scientist II (Kettner), Institute of Arctic and Alpine Research, University of Colorado, Boulder, Colorado 80309; Currently GIS & Water Resources Specialist (Bates), NOAA National Water Center, Lynker Technologies, Tuscaloosa, Alabama 35401; Research Hydrologist (Nelson) and Hydrologist (McDonald), Geomorphology and Sediment Transport Laboratory, U.S. Geological Survey, Golden, Colorado 80403; Graduate Student (Huang), Department of Natural Resources and Environmental Management, University of Hawaii at Manoa, Manoa, Hawaii 96822; and Graduate Student (Zhang), Department of Civil and Environmental Engineering, University of Texas, Arlington, Texas 76019 (E-Mail/Cohen: sagy.cohen@ua.edu).

resolution maps for specific floods. Copernicus provides on-demand flood inundation maps based on available high-resolution imagery. A more recent service, the United States Flood Inundation Mapping Repository (USFIMR) (Accessed August 1, 2017, <http://sdml.ua.edu/usfimr>), provides high-resolution (10-30 m) satellite sensor-based map repository (40 maps as of August 1, 2017) of past flood events in the United States (U.S.).

Near-real-time observations of flood extent are useful for first responders, relief agencies, civil leaders, and recovery managers (Horritt *et al.*, 2007; Merz *et al.*, 2007; Schumann *et al.*, 2010; Mason *et al.*, 2012). Detailed maps of past flood events can be useful for flood risk policymakers as well as for scientists developing and maintaining modeling-based flood prediction and analysis applications (Hostache *et al.*, 2009; Revilla-Romero *et al.*, 2015).

Flood inundation maps provide information on the areal extent of a flood. With the exception of very small, *i.e.*, easily surveyed, floods, water depth cannot be readily associated with or calculated from a flood extent map. However, timely information about floodwater depth is important for directing rescue and relief resources, determination of road closures and accessibility, and post-event analysis of property damage (Islam and Sadu, 2001; Nadal *et al.*, 2009).

Hydraulic models, for example, HEC-RAS (USACE, 2017), Delft3D (Deltares, 2017), MIKE FLOOD (DHI Technologies, 2017), and LISFLOOD-FP (Bates and De Roo, 2000), are commonly used to simulate flooding events (*e.g.*, Horritt and Bates, 2002; Haile and Rientjes, 2005; Kia *et al.*, 2012; Xu *et al.*, 2016). Although these tools can simulate water depths, they require information about the event hydrological characteristics and riverine morphology. Achieving accurate simulation of a flood event is often time consuming and requires extensive data compilation and calibration. As a result, numerical simulations are less frequently used in near-real-time flood mapping application. Model-based flood mapping applications [*e.g.*, Federal Emergency Management Administration Flood Maps (FEMA, 2017) and the National Oceanic and Atmospheric Administration/National Weather Service Inundation Maps (NOAA, 2017)] often analyze flow frequency or stage intervals or past flow conditions at a gauging site which makes them less useful for near-real-time or event-specific applications.

The objective of this paper is to introduce and test a new methodology for estimating water depths in flooded domains that relies on only flood extent and a digital elevation model (DEM). We test whether our methodology can provide a comparable estimate of floodwater depth to a complex hydrologic model. The methodology uses standard geographic information

system (GIS) tools within a simple Python script, termed the Floodwater Depth Estimation Tool (FwDET). The relative simplicity of FwDET allows for fast calculation of floodwater depth using readily available data, a highly desirable attribute for near-real-time flood mapping applications or systems that analyze a large number of flood events (*e.g.*, USFIMR). The approach is intended for first-order overview, not detailed analysis of floodwater dynamics. In this paper, we present the methodology and test it against two case studies for which water depth maps are available from hydraulic simulations. We then demonstrate the tool for two additional flood inundation maps from the DFO and USFIMR databases.

METHODOLOGY

Floodwater Depth Estimation Approach

Water depth along a cross section of a floodplain (Figure 1) can be easily estimated by extracting the maximum elevation of the water surface from a DEM and deducting the elevation of any location along the cross section, assuming negligible cross-valley water surface slope. In Figure 1, for example, the maximum elevation of the floodwater is 100 m above sea level (asl). At point “A” along the cross section, the land elevation is 95 m asl, leading to an estimated water depth of 5 m. Above the river channel (point “B”), underestimation of water depth will occur if the DEM records the river water surface elevation (the blue line in Figure 1) rather than river bed elevation. As most DEMs reflect water surface elevation (at some point in time) over the active channel, this bias will be persistent and may be considerable, especially for large rivers. It is however of little importance in

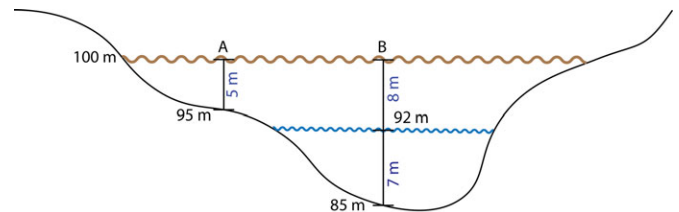


FIGURE 1. Theoretical Floodplain Cross Section Illustrating the Floodwater Depth Estimation. The blue line represents “within banks” water level, and the brown line represents hypothetical floodwater level. Once the local elevation of floodwater is identified (100 m asl in this example), the floodwater depth can be estimated at any point using the difference in surface flood water elevation and inundated land elevation (*e.g.*, $100 - 95 \text{ m} = 5 \text{ m}$). For the river channel, the accuracy of this methodology depends on whether or not the digital elevation model records the elevation of the riverbed or the water surface.

practice, as *e.g.*, first responders' primary concerns are with water depths over flooded areas, not the active channel.

Using cross-section maximum floodwater elevation value for estimating water depth cannot be directly applied for larger areal extents due to the slope of the floodplain and, for some cases, the complexity in flow paths. Delineating multiple cross sections along a flooded extent and interpolating between them can, however, yield more continuous water depth estimations. That approach will be sensitive to the spacing between the cross sections and flow complexity, such as river meandering, confluences, and distributaries, but has potential given emerging algorithms that can automate cross-section delineation (*e.g.*, HEC-GeoRAS) and interpolation (*e.g.*, Merwade *et al.*, 2008).

The method described herein allows for an automated floodwater depth estimation that is spatially continuous (*i.e.*, not based on cross sections). It (Figure 2) is based on identifying the flooded domain boundary cells on a DEM, using a polygon layer delineating the flood extent obtained, for example, from remote sensing classification. The elevation values of the boundary cells are then assigned to cells within the flooded domain. This extraction of the local maximum floodwater elevation, as in the simple cross-section example, can be used to calculate water depth within the flooded domain. To accomplish this, a cell within the flooded domain will be assigned the elevation of its nearest boundary cell, which is then used to calculate the local water depth by subtracting this value from a cell's surface elevation (derived from a DEM). The methodology was automated using a Python script (FwDET) utilizing a number of ArcGIS tools (within the ArcPy Python library). Other geospatial analysis packages (GDAL) (*e.g.*, <http://www.gdal.org>) can also be used for executing this method.

The method includes the following sequence (Figure 2).

Step 1 — Identifying Boundary Cells. A flood inundation extent polygon is converted into a polyline layer (ArcGIS "Polygon to Polyline" tool). The polyline layer is then converted into a raster layer (ArcGIS "Polyline to Raster" tool), with cells that are not corresponding to the polylines assigned with a "No Data" value (Figure 2a). It is preferable to have the raster layer cell dimensions compatible to the available DEM (Figure 2b). If the initial inundation map is a raster (*e.g.*, tiff, kmz), which is sometimes the case, that map needs to be converted into a polygon before being converted into a polyline. When the inundation extent layer is composed of multiple polygons or when there are holes within the polygons, the

boundaries of these will also be identified as boundary cells. The case studies used in this paper include such complex flood extents. The output of this step is a raster of the flooded area, with all cell values equal to "No Data" except for cells representing the polyline (Figure 2a).

Step 2 — Extracting the Elevation of the Boundary Cells. A new raster layer is generated, using a conditional raster calculation (ArcGIS Map Algebra) expression, in which cells corresponding to the boundary raster layer (from Step 1), which are not "No Data," receive the value of the underlying DEM (Figure 2c).

Step 3 — Assigning the Boundary Cells Elevation to the Domain Cells. A new raster layer is calculated in which each cell is assigned with the elevation of its nearest boundary cell. In FwDET, the "Focal Statistics" tool is used (ESRI, 2017). The tool calculates a selected statistic for each input cell of the values within a specified neighborhood around it. For example, for the output of Step 2 (Figure 2c) with a "Focal Statistics" neighborhood of one cell, only the adjacent cells to the boundary cells will be assigned the elevation of their nearest boundary cell (Figure 2d). This is because all other cells are surrounded by "No Data" cells. To ensure that all cells are assigned with the elevation of their nearest boundary cell, a conditional loop is used in which the size of the "Focal Statistics" neighborhood is increased at every iteration (Figures 2d and 2e). The loop is conditioned in a way that the value of a cell in the new raster layer will be assigned the elevation value of the smallest neighborhood (iteration) size, *i.e.*, the nearest boundary cell. A circular "Focal Statistics" neighborhood was found to produce smoother results, but other neighborhood geometries can also be used. The number of iterations needed is a function of the maximum flood extent width and the cell size used. It can be calculated by identifying the largest flood extent width and dividing it by the cell size times 2 (as it only needs to reach the middle of the flood extent from each side). For example, for a flood extent with a maximum width of 1,000 m and the DEM resolution is 10 m, at least $(1,000/[2 \times 10])$ 50 iterations will be needed.

Step 4 — Floodwater Depth Calculation. A raster calculation (ArcGIS Map Algebra) expression is used to deduct the cell value of the output of Step 3 (a raster layer containing the elevation of the nearest boundary cell; Figure 2e) by the DEM value (Figure 2b). The values of the resulting raster layer will be the estimated floodwater depth (Figure 2f). The DEM used in this step needs to be bounded to only

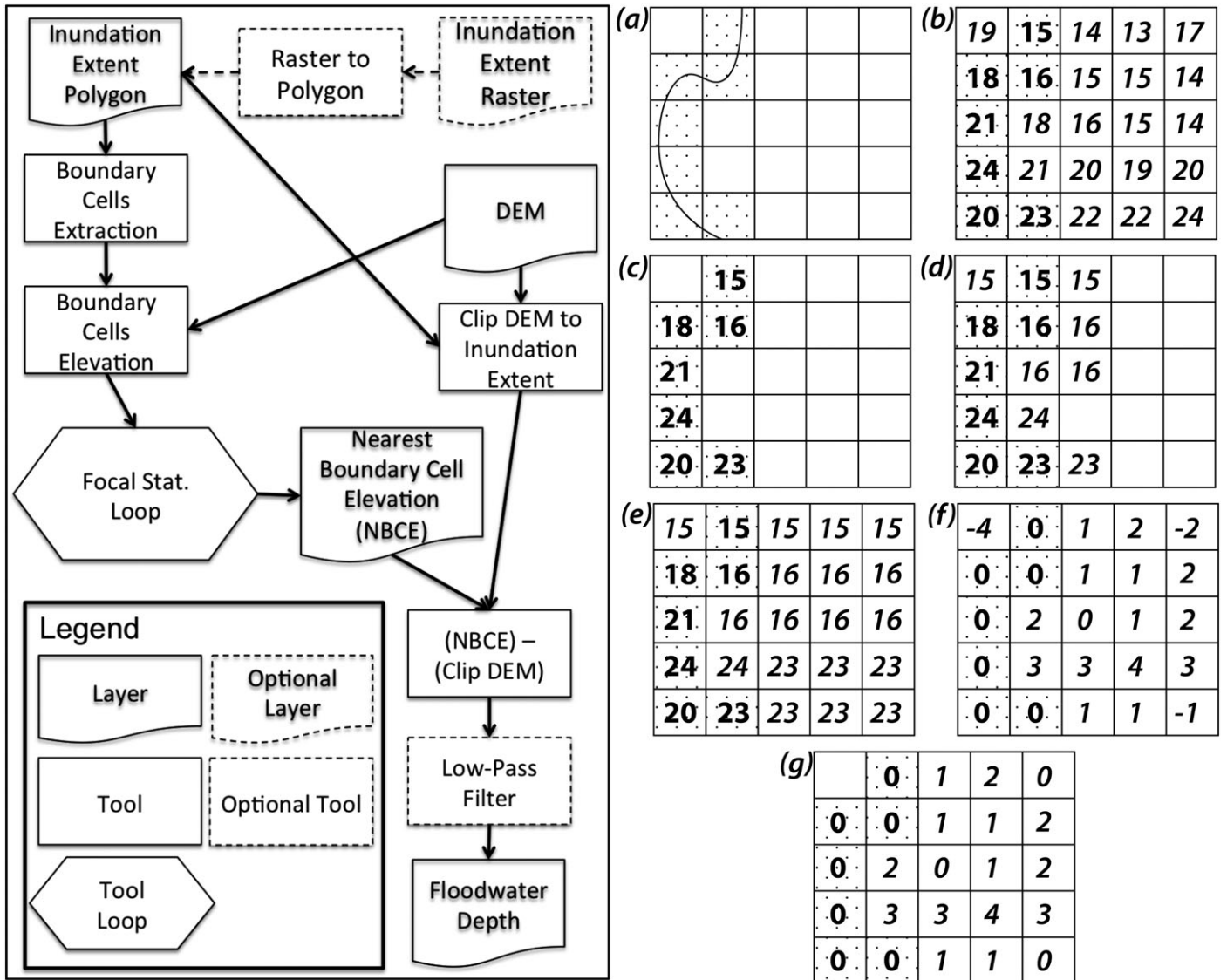


FIGURE 2. Flow chart of the Floodwater Depth Estimation Methodology (left panel) and Illustration of the FwDET Calculation. (a) Zoom-in on flood inundation boundary section (line) and corresponding grid-cells (dotted cells); (b) digital elevation model (DEM) values (above sea level); (c) boundary cells elevation (asl) extraction from the DEM; (d) first iteration of the focal statistics loop which assign the nearest boundary cell elevation to 1 cell-wide neighborhood; (e) final iteration of the focal statistics loop, all cells are assigned with elevation of the nearest boundary cell; (f) calculation of water depth by deducting (e) from (b); (g) negative water depth values and cells outside the flooded domain are removed.

include cells within the flooded domain (Figure 2g). In FwDET, the Clip tool is used with the flood extent polygon as the bounding feature. This step is necessary because the “Focal Statistics” tool assigns values on both sides of the boundary cells.

Step 5 — Smoothing. A procedure can be used to smooth sharp changes in floodwater depth due to, for example, spatial mismatches between the DEM and the inundation map. This step can also smooth real, sharp changes in water depth, such as transition from floodplain to active channel, and so discretion should be used when analyzing the output of

this step. In FwDET, the “Filter” tool is used with the “low-pass” option. The tool calculates the average value for each cell based on its 3×3 neighborhood.

Evaluation and Application Examples

The methodology was evaluated by comparing the FwDET floodwater depth output layer against water depths simulated by a hydraulic model for two flood events: May 2016 at Brazos River, Texas, U.S., and September 2013 at St. Vrain Creek near Lyons, Colorado, U.S. These two events represent very different

flooding conditions and input data. The Brazos River event was spatially extensive (width of about 4.5 km) and a 10 m resolution DEM is used as input. The St. Vrain Creek was a small and relatively confined (width of about 0.3 km), mountainous, flood and a 1 m resolution, LiDAR-derived, DEM (FEMA Region VIII GIS FTP Site, 2014) was used as input. In both cases, the iRIC-FaSTMECH model (Nelson *et al.*, 2016) (www.i-ric.org) was used to simulate the floods. Model-predicted water depth output is used to evaluate FwDAT. iRIC-FaSTMECH employs a channel-fitted coordinate system and calculates either two-dimensional or three-dimensional velocity fields and water surface elevations for a given discharge and roughness field assuming that the pressure distribution is hydrostatic and that the flow is quasi-steady (where quasi-steady means that the discharge can vary in time, but unsteady terms in the equations of motion are neglected). Notably, the iRIC system includes a variety of additional flow models with less restrictive assumptions and more general applicability. FaSTMECH was selected because it is fast to simulate flow, easy to use, and favorable with limited amount of gage data.

Model-predicted flood inundation area is used as the flood extent input layer in FwDAT, serving as a substitute to an observed inundation map. Using model-predicted flood extent input allows for a cleaner analysis of our methodology, as it removes model-related errors from the analysis and ensures that the differences between FwDAT and the hydraulic model simulated water depths are only due to the simplifications in FwDAT and not due to differences in input data.

FwDET predictions are also demonstrated for two satellite-observed flood inundation events. The first is a DFO map for the August 2016 flood event on the Irrawaddy River in Myanmar (Accessed August 1, 2017, <http://floodobservatory.colorado.edu/Events/2016Myanmar4365/2016Myanmar4365.html>), using 250 m spatial resolution MODIS imagery. DFO MODIS classification was based on the Land Atmosphere Near-real-time Capability for EOS (LANCER) system that provides daily MODIS. The MODIS inundation extent information is further processed at DFO from a fully automated, near global, near real-time surface water extent and flood mapping system (<https://floodmap.modaps.eosdis.nasa.gov/>). The system has been running at NASA's Goddard Space Flight Center (GSFC) since November 2011 and ingests data from the MODIS sensors on both the NASA Aqua and Terra satellites. Water is identified using the 250 m spatial resolution red (MODIS Band 1) and near infrared bands (MODIS band 2) data. A band threshold classification approach uses the low water reflectivity in band 2 as ratioed against band 1

to identify "water," and then further removes cloud shadow false positives by requiring the "water" threshold to be met in three of the six images available from Terra and Aqua for a three-day period (Policelli *et al.*, 2016). The automated system then rolls forward in time, updating daily. For obtaining maximum flood extent maps, DFO commonly also composites over longer time periods (14 days is typical), thus filling between cloud cover and obtaining the maximum extent of flooding reached. A 3 arc-sec (~90 m) resolution DEM (HydroSHEDS) (Lehner *et al.*, 2008) is used as input topography.

The second event is a USFIMR map for the May 30, 2016 flood on the San Jacinto River, Texas using 10 m Sentinel-1 (synthetic aperture radar; European Space Agency) imagery. The Sentinel-1 imagery was downloaded from the Copernicus Open Access Hub (Accessed August 1, 2017, <https://scihub.copernicus.eu/>). Flood extent was classified, using a change detection approach in which the difference between an image during the flood is compared to a pre-flood image. Before and after images were processed using the Sentinel-1 Toolbox (<https://sentinel.esa.int/web/sentinel/toolboxes/sentinel-1>). Images underwent filtering, radiometric calibration, and geometric correction before a threshold was used to create binary classifications of wet/dry pixels. The classification threshold was determined through visual inspection of backscatter fluctuations in the pre- and post-flood imagery.

The effects of DEM resolution on FwDET predictions are evaluated by comparing floodwater depth predictions for the San Jacinto River, Texas, case study, using 10 and 30 m resolution DEMs (from USGS National Elevation Dataset; Accessed September 1, 2016, <https://lta.cr.usgs.gov/NED>) for the floodwater depth estimation. These case studies were selected as they include a number of diverse features. The Myanmar flood passes through a narrow valley into a large floodplain and is based on relatively coarse resolution mapping. The San Jacinto River flood included a large reservoir, urban flooding, and highly dispersed inundated areas.

RESULTS AND DISCUSSION

Evaluation of FwDET

FwDET runtime on a desktop computer with four 3.7 GHz processors and 7.5 GB available RAM varied from 3.6 min for the St. Vrain Creek case study, with a 1 m resolution, 640 × 615 (393,600) cells and 100 iterations, to 31.7 min for the Brazos River case

study, with a 10 m resolution, 2087×1816 (3,789,992) cells and 200 iterations. Runtime is a function of the input data resolution and the size of the flood inundation domain relative to the DEM resolution. The former affects the time it takes to execute each operation (tool) and the latter controls the number of integrations needed for the “Focal Statistic” neighborhood to cover all grid-cells within the flooded domain. We plan to test other tools and other geospatial analysis packages (e.g., GDAL; <http://www.gdal.org>) to improve runtime and usability by non-ArcGIS users.

Floodwater depth estimates by FwDET correspond well with model-simulated water depth for the Brazos River, Texas (Figures 3a and 3b, respectively). The average depths estimated by our methodology and the model (including cells with zero depth but excluding “No Data” cells) are 1.95 and 1.49 m, respectively. The root-mean-square difference (RMSD; the average absolute difference between all cells between the two water depth maps) is 0.37 m. Maximum depths estimated by FwDET and the hydraulic model were 12.4 and 12.5 m, respectively. These results are favorable

as it shows that FwDET estimates deviate from a calibrated hydraulic model floodwater depth estimation by <40 cm on average for a flood with a maximum water depth of over 12 m. While local discrepancies between the two can be significant, as we describe below, such a low average bias and the ability to capture the maximum floodwater depth is promising.

While most of the flooded area shows small (<0.5 m) differences in water depth between the two maps, some small sections show considerable differences (Figures 3c and 3d). The most extreme overestimations by FwDET (green values in Figure 3d) are along the banks of the main river channel. These are due to FwDET’s inability to calculate fine-scale fluid dynamic effects. The greatest differences (>5 m) in floodwater predictions are the underestimation by FwDET at the up- and down-stream boundaries of the river reach (Figure 3d). This is a result of using the edges of the flooded domain that cross the river channel as boundary cells to the nearby cells within the river channel. As a result, FwDET calculates very low water depth at these cells (their “reference” boundary cells are also within the channel), whereas

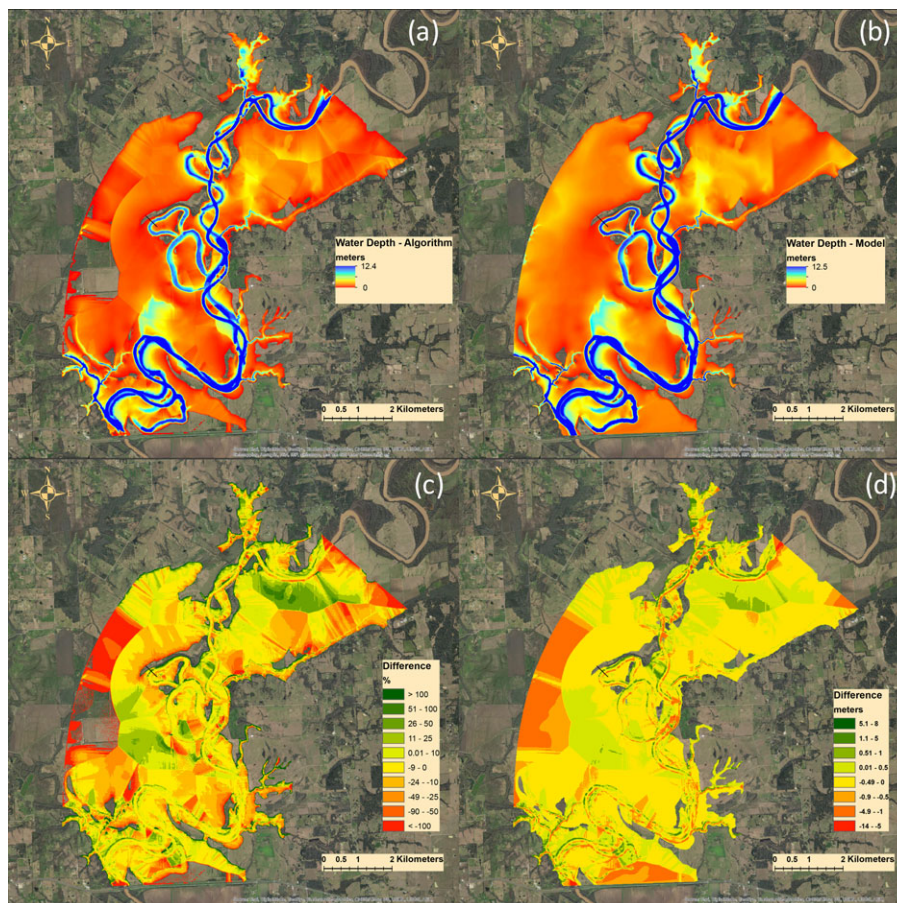


FIGURE 3. May 2016 Flood Event at the Brazos River, Texas, U.S. (a) Estimates by FwDET and (b) simulated by the iRIC-FaSTMECH hydraulic model. Differences between (a) and (b) are shown as a (c) percentage and (d) in depth of meters. Negative or positive values indicate that floodwater depth estimates by FwDET were lower or higher than model predictions.

the model properly accounts for these boundary locations. Given the small number of cells affected by this problem and their location within the river channel, this bias does not greatly influence the utility of the floodwater depth estimate.

The floodwater depth estimation by FwDET (Figure 3a) shows sharp transitions (most clearly visible in Figure 3c) in depth, in contrast to the smoother distribution of the modeled depth map (Figure 3b). These blocks and straight lines are artifacts of the Focal Statistics circular neighborhood. The low-pass filter step smooths these artifacts but does not eliminate them. Additional filtering passes and algorithms could be used but these may have adverse effects on capturing actual sharp transitions in water depth (e.g., from the floodplain to the active channel).

Floodwater depth estimates by FwDET also correspond well to the small-scale and high-resolution St. Vrain Creek event simulation (Figure 4). The average floodwater depth estimated using FwDET and model-simulated depths (including cells with zero depth) are 0.72 and 1.28 m, with maximum depths of 4.64 and 4.26 m, respectively, and an RMSD of 0.38 m. The

RMSD value is very similar to the Brazos River case study. However, it represents a more considerable bias as the average and maximum floodwater depths are smaller. This is, nonetheless, a promising result as it shows consistency in FwDET predictions between two case studies at considerably different spatial scales and resolution. The greatest differences in floodwater depth between the two maps are at the most upstream and downstream edges of the simulated domain (Figure 4d). FwDET underpredicts floodwater depth in these locations by up to 2 m. Similar to the Brazos River flood, this is due to the identification of cells at the edge of the inundation domain that are within the active channel and have lower elevation as boundary cells.

Differences between the two floodwater depth maps (Figures 4a and 4b) are highly heterogeneous in space (Figures 4c and 4d). This highlights the effect of boundary cell location on the resulting floodwater depth estimation. Complex flood inundation domains will typically yield more “bulky” estimations because these flood domains are more likely to have boundary cells with relatively high differences in

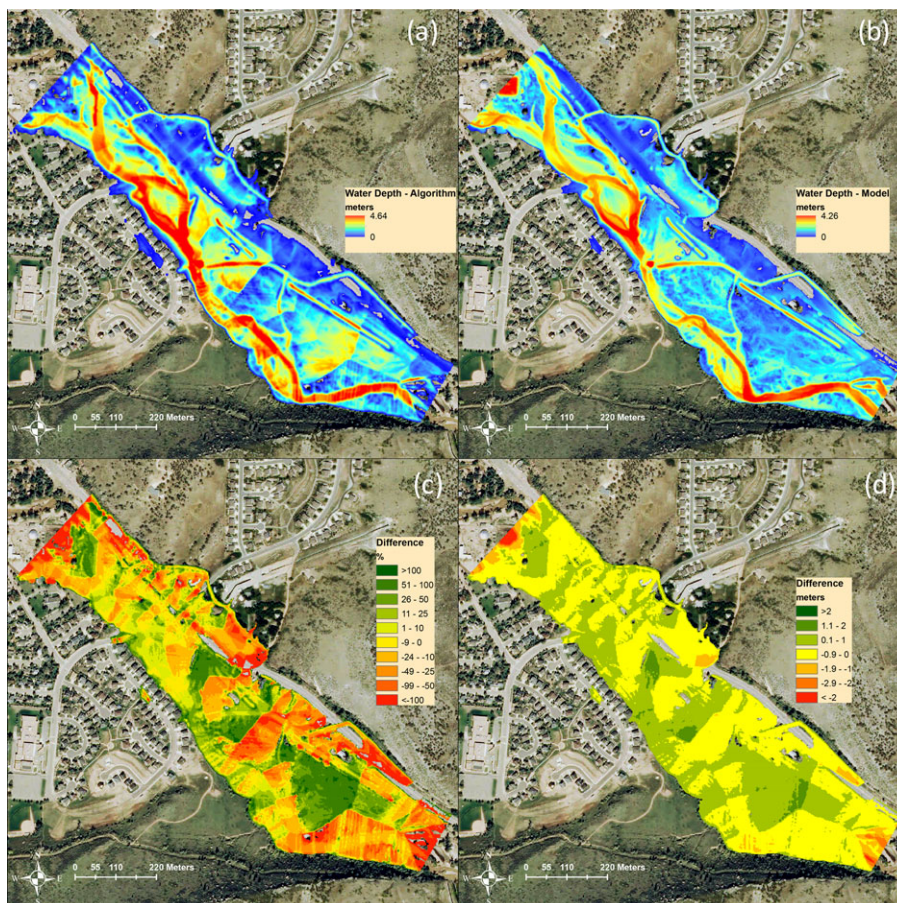


FIGURE 4. September 2013 Flood Event at St. Vrain Creek near Lyons, Colorado, U.S. (a) Estimates by FwDET and (b) simulated by the iRIC-FaSTMECH hydraulic model. Differences between (a) and (b) are shown as a (c) percentage and (d) depth in meters. Negative or positive values indicate that floodwater depth estimates by FwDET were lower or higher than model predictions.

elevation at close proximity. For example, the “holes” along the inundated area (best seen in Figure 4c) are associated with regions of large differences between the two floodwater depth predictions. A smoothing procedure could be added to FwDET that will remove such “holes” within the inundated domain, but this may have adverse effects for large floods, where the distance between boundary cells and cells within the flooded domain can be very large. Thus, an “island” within the flooded domain may yield a more accurate, local estimate of floodwater elevation.

Demonstration for Remote Sensing Flood Maps

The Irrawaddy River (Myanmar) case study yielded unrealistic floodwater depth values at the upstream (northeastern) section of the river (Figure 5a). The river is confined within a narrow valley along that reach. The relatively coarse resolution of the MODIS-based water classification (white outline in Figure 5c) and the DEM resulted in boundary cells identification near the top of the valley ridges (with very high elevation). This demonstrates that the spatial resolution of the input data (DEM and inundation map) should be appropriate to the flood extent and floodplain characteristics. Higher-resolution data or manual quality control would allow for a better assessment of water depth in this section of the river.

One of the adverse effects of the overestimation of floodwater depth along the upstream section of the Irrawaddy River is the masking of depth values along the downstream section of the flood (due to “color ramp” saturation). Focusing on the middle and lower sections of the flood (Figure 5b), a complex mosaic of deep and shallow sections emerges. Many of these variations are due to the braided nature of the river (Figure 5c) and may realistically represent floodwater depths. There are a number of straight transition zones, mostly perpendicular to the flow direction. Similar to earlier examples, these are artifacts of the Focal Statistics neighborhood, which in this case resulted in a number of alternating deep-shallow zones which are not realistic. The resolution of the inundation map and DEM also played a role in this as boundary cells may have been located slightly outside the active floodplain, which introduced high elevation values in some locations. This, again, demonstrates the importance of using suitable input data resolution and the need for quality control in some locations. It also demonstrates the sensitivity of our approach to spatial mismatch between the flood inundation extent layer and the DEM. Such mismatch can result not only from relatively coarse spatial resolution but also from projection or grid-cell alignment issues.

The San Jacinto River, Texas, U.S., case study includes flooding along Lake Houston, a large reservoir, coastal wetlands, and urban environments. Much of the reservoir surface was estimated as having zero floodwater depth despite the fact the areas surrounding the reservoir were classified as flooded (Figure 6). This occurred in areas where one or more boundary cells were located, due to errors in the remote sensing-based map, on the reservoir itself. Most of the sections of the reservoir that were calculated as having some floodwater depth show unrealistic bands resulting from the applied Focal Statistics neighborhood algorithm. This, again, demonstrates how spatial mismatches between the flood inundation extent layer and DEM can lead to evident biases in floodwater depth estimates. Careful flood extent quality control and manual adjustment of the boundary cell locations can improve these biases. Narrow parts of the reservoirs upstream (north and northwest areas) show more realistic floodwater depth patterns. In all cases, it is clear that the DEM used recorded the water surface elevation, rather than the reservoir bed elevation, leading to considerable underestimation of water depth over the reservoir. While this issue points to a potential source of bias, its importance may be considered low as the main use of this tool is to provide a first-order estimate floodwater depth over the floodplain, where the potential impact of flood events on life and property is more likely.

The northwest (upstream) area of the flood shows complex inundation patterns along streets and neighborhoods (*e.g.*, checkered box in Figure 6). The estimated floodwater depth in these locations is low (~1 m). There are isolated areas of very deep floodwater hotspots. These were the result of (1) errors in the location of boundary cells due to either imagery misclassification or the spatial resolution of the satellite imagery, and (2) areas of low elevation associated with small ponds or ditches. These kinds of errors are more likely to occur in complex flood inundation patterns like this one. Using a higher resolution DEM (10 m; Figure 6a) improves the results for this section, primarily by providing additional detail that reduces the spatial extent of these deeper hotspots.

The downstream section of this flood (south section below the dam) is a flat coastal wetland incised by a meandering river. The estimated floodwater depth for this section (red box in Figure 6) is reasonable but is very irregular when using the 10 m DEM, with sharp transition in water depth. The 30 m DEM resulted in much smoother output which may be preferable for floodwater depth reporting in this case.

The overall differences between the 10 and 30 m results (Figures 6a and 6b, respectively) are relatively small. The average floodwater depths estimated

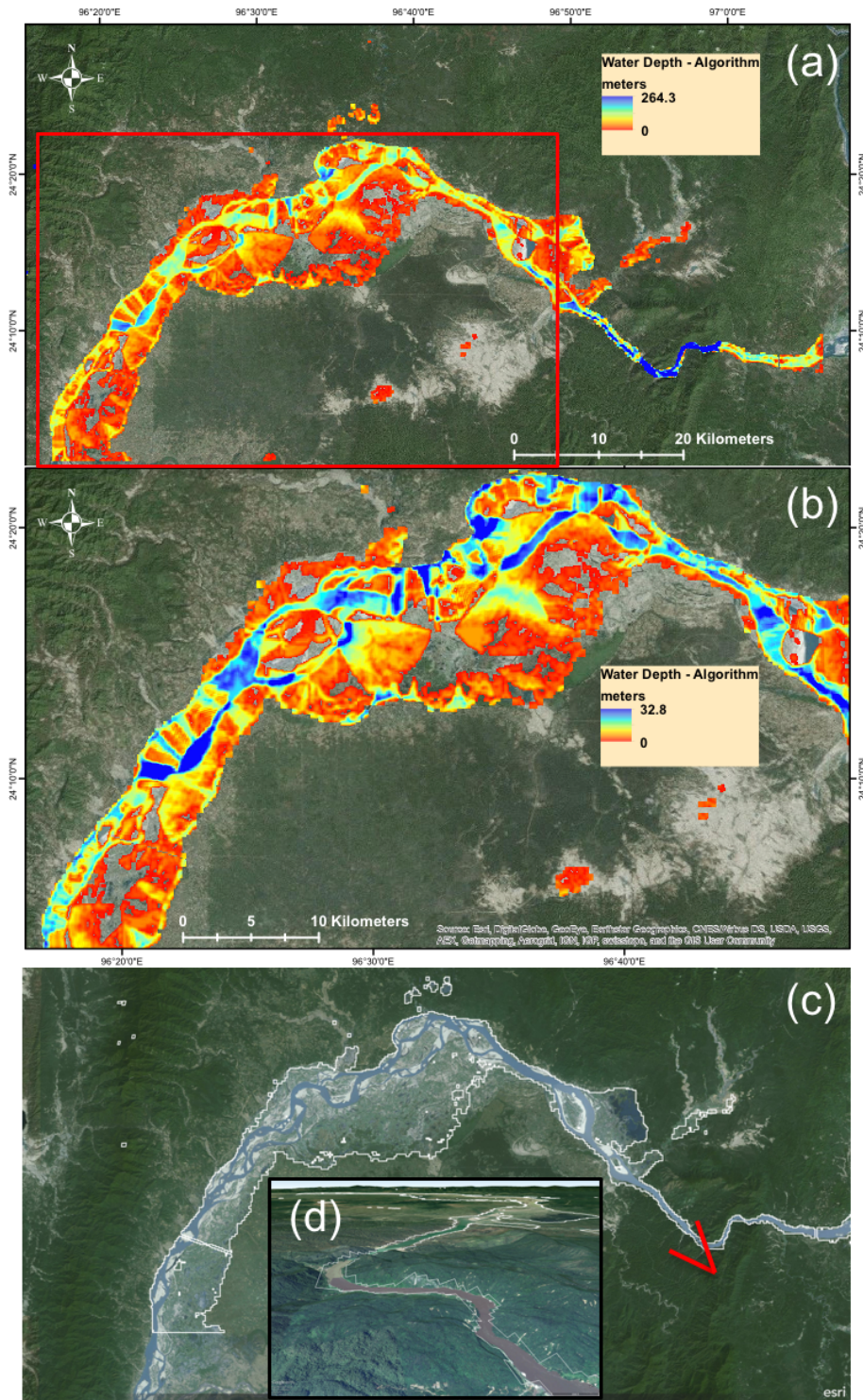


FIGURE 5. The August 2016 Flood Event at Irrawaddy River, Myanmar: (a) Floodwater Depth Prediction by FwDET, (b) Zoom-in on the Section Downstream of the Gorge (indicated by the red rectangle in (a)), (c) Satellite Imagery (from ArcGIS Earth) of the Flood Zone and the Moderate Resolution Imaging Spectroradiometer-Based Flood Inundation Extent (marked in white), (d) Oblique View from the Upstream Gorge (view angle indicated by red cone in (c); from Google Earth).

are 0.75 and 1.25 m, with the maximum depths being 11.7 and 13.3 m for the 10 and 30 m DEMs, respectively. As described earlier, high-resolution analysis

is advantageous in complex urban settings but can also be disadvantageous in some cases. Given that the goal of the described method is to provide a first-

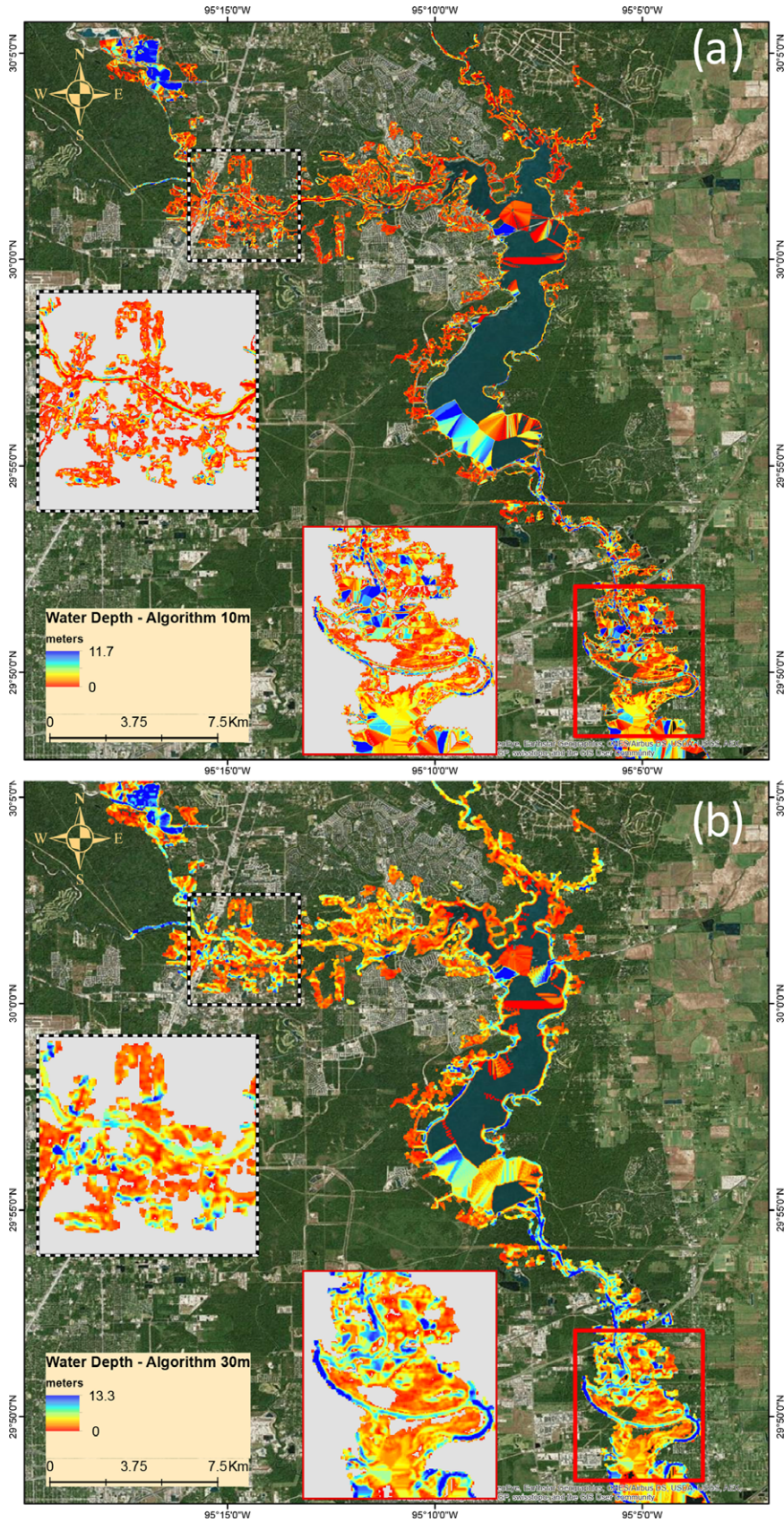


FIGURE 6. Floodwater Depth Estimates from FwDET for the May 2016 Flood Event at San Jacinto River, Texas, U.S., Using (a) a 10×10 m DEM and (b) a 30×30 m DEM. The small maps zoom in on an urban area (top map inset) and wetland area (bottom map inset).

order overview of floodwater depth, and not a precise analysis, the use of higher spatial resolution DEMs should not be expected to improve the results significantly.

CONCLUSIONS

A new methodology, the FwDET, is presented for the important challenge of estimating floodwater depth from remote sensing flood inundation maps. When compared to model-simulated water depth predictions, FwDET performs well for both a large flood event (Brazos River, Texas; using a 10 m DEM) and a small event (St. Vrain River, Colorado), for which high-resolution 1 m DEM was used.

FwDET was also demonstrated, using two satellite remote sensing-derived flood inundation maps. These flood maps feature a number of challenges, including a narrow valley, a large reservoir, urban flooding, and braided and meandering channels. The main conclusions from that analysis were as follows:

1. Steep terrain (e.g., narrow valley) may lead to considerable overestimations as they are highly sensitive to the resolution of the flood inundation map and DEM. Highly confined river reaches should be excluded unless appropriate (high resolution) input data are available and/or careful manual quality control is implemented to ensure accurate spatial alignment between the flood inundation layer and the DEM.
2. Large water bodies are prone to underestimation due to errors in the location of the flood boundary cells on the water body itself and the fact that DEMs typically record water surface elevation. Large river channels will show similar biases. Manual quality control should be used to prevent the former, whereas bathymetry estimations can address the latter.
3. Complex inundation patterns and urban flooding are prone to localized hotspots of overestimation. Higher quality imaging and DEM inputs are found to limit the spatial extent of these hotspots. Appropriate DEM resolution selection is needed to produce the best estimation under these settings.

Future research will focus on testing other tools and geospatial analysis packages to improve runtime and usability by non-ArcGIS users. We plan to further test FwDET using observed water depth from sources such as the USGS High Water Mark (HWM) data (USGS, 2017). Immediately, however, we will

use FwDET to provide floodwater depth estimates for remote sensing products at the USFIMR and DFO portals. The tool Python script is available at the Surface Dynamics Modeling Lab (SDML) Models portal (<https://sdml.ua.edu/models/>) and the Community Surface Dynamics Modeling System (CSDMS) Model Repository (http://csdms.colorado.edu/wiki/Model_download_portal).

ACKNOWLEDGMENTS

This research was funded as part of the USFIMR project grant from the University Corporation for Atmospheric Research (UCAR) COMET Program for the National Water Center (NWC) Cooperative Project Grant under Cooperative Agreement No. Z16-23487 with the National Oceanic and Atmospheric Administration (NOAA). Part of this work was conducted during the 2016 NWC Summer Institute. Cohen was partly funded by a grant from the National Science Foundation (NSF) via Award #1561082. Brakenridge and Kettner thank the National Aeronautics and Space Administration (NASA) for its support via grant NNX15AG85G. Any use of trade, firm, or product name is for descriptive purposes only and does not imply endorsement by the United States Government.

LITERATURE CITED

- Bates, P.D. and A.P.J. De Roo, 2000. A Simple Raster-Based Model for Flood Inundation Simulation. *Journal of Hydrology* 236 (1):54-77, [https://doi.org/10.1016/S0022-1694\(00\)00278-X](https://doi.org/10.1016/S0022-1694(00)00278-X).
- Deltares, 2017. Delft3D Open Source Community. <https://oss.deltares.nl/web/delft3d/home>.
- DHI Technologies, 2017. MIKE FLOOD. <https://www.mikepoweeredbydhi.com/products/mike-flood>.
- ESRI, 2017. ArcGIS for Desktop – Focal Statistics. <http://desktop.arcgis.com/en/arcmap/10.3/tools/spatial-analyst-toolbox/focal-statistics.htm>.
- FEMA (Federal Emergency Management Agency), 2017. FEMA Flood Map Service Center. <https://msc.fema.gov>.
- FEMA Region VIII GIS FTP Site, 2014. Colorado Flooding 2013.
- Haile, A.T. and T.H.M. Rientjes, 2005. Effects of LiDAR DEM Resolution in Flood Modelling: A Model Sensitivity Study for the City of Tegucigalpa, Honduras. *Isprs wg III/3, III/4, 3, Workshop, Enschede, Netherlands, September 12-14*, pp. 168-173.
- Horritt, M.S. and P.D. Bates, 2002. Evaluation of 1D and 2D Numerical Models for Predicting River Flood Inundation. *Journal of Hydrology* 268(1):87-99. [https://doi.org/10.1016/S0022-1694\(02\)00121-X](https://doi.org/10.1016/S0022-1694(02)00121-X).
- Horritt, M.S., G. Di Baldassarre, P.D. Bates, and A. Brath, 2007. Comparing the Performance of a 2-D Finite Element and a 2-D Finite Volume Model of Floodplain Inundation Using Airborne SAR Imagery. *Hydrological Processes* 21(20):2745-2759, <https://doi.org/10.1002/hyp.6486>.
- Hostache, R., P. Matgen, G. Schumann, C. Puech, L. Hoffmann, and L. Pfister, 2009. Water Level Estimation and Reduction of Hydraulic Model Calibration Uncertainties Using Satellite SAR Images of Floods. *IEEE Transactions on Geoscience and Remote Sensing* 47(2):431-441, <https://doi.org/10.1109/TGRS.2008.2008718>.
- Islam, M.M. and K. Sadu, 2001. Flood Damage and Modelling Using Satellite Remote Sensing Data with GIS: Case Study of

- Bangladesh. In: J. Ritchie, *et al.* (Editors), Remote Sensing and Hydrology 2000, IAHS Publication, Oxford, pp. 455-458.
- Kia, M.B., S. Pirasteh, B. Pradhan, A.R. Mahmud, W.N.A. Sulaiman, and A. Moradi, 2012. An Artificial Neural Network Model for Flood Simulation Using GIS: Johor River Basin, Malaysia. *Environmental Earth Sciences* 67(1):251-264. <https://doi.org/10.1007/s12665-011-1504-z>.
- Lehner, B., K. Verdin, and A. Jarvis, 2008. New Global Hydrography Derived from Spaceborne Elevation Data. *Eos, Transactions American Geophysical Union* 89(10):93-94, <https://doi.org/10.1029/2008EO100001>.
- Mason, D.C., I.J. Davenport, J.C. Neal, G.J.P. Schumann, and P.D. Bates, 2012. Near Real-Time Flood Detection in Urban and Rural Areas Using High-Resolution Synthetic Aperture Radar Images. *IEEE Transactions on Geoscience and Remote Sensing* 50(8):3041-3052, <https://doi.org/10.1109/TGRS.2011.2178030>.
- Merwade, V., A. Cook, and J. Coonrod, 2008. GIS Techniques for Creating River Terrain Models for Hydrodynamic Modeling and Flood Inundation Mapping. *Environmental Modelling & Software* 23(10):1300-1311, <https://doi.org/10.1016/j.envsoft.2008.03.005>.
- Merz, B., A.H. Thielen, and M. Gocht, 2007. Flood Risk Mapping at the Local Scale: Concepts and Challenges, in Flood Risk Management in Europe: Innovation in Policy and Practice. In: Advances in Natural and Technological Hazards Research, S. Begum, M.J.F. Stive, and J.W. Hall (Editors). Springer, Dordrecht, The Netherlands, pp. 231-251.
- Nadal, N.C., R.E. Zapata, I. Pagán, R. López, and J. Agudelo, 2009. Building Damage due to Riverine and Coastal Floods. *Journal of Water Resources Planning and Management* 136(3):327-336.
- Nelson, J.M., Y. Shimizu, T. Abe, K. Asahi, M. Gamou, T. Inoue, T. Iwasaki, T. Kakinuma, S. Kawamura, I. Kimura, and T. Kyuka, 2016. The International River Interface Cooperative: Public Domain Flow and Morphodynamics Software for Education and Applications. *Advances in Water Resources* 93:62-74, <https://doi.org/10.1016/j.advwatres.2015.09.017>.
- NOAA, 2017. Advanced Hydrologic Prediction Service (AHPS). <http://water.weather.gov/ahps/inundation.php>.
- Policelli, F., D. Slayback, B. Brakenridge, J. Nigro, A. Hubbard, B. Zaitchik, M. Carroll, and H. Jung, 2016. The NASA Global Flood Mapping System. In: Remote Sensing of Hydrological Extremes, V. Lakshmi, and G. Huffman (Editors). Springer International Publishing, Switzerland 2017, ISBN 978-3-319-43743-9.
- Revilla-Romero, B., F.A. Hirpa, J.T.D. Pozo, P. Salamon, R. Brakenridge, F. Pappenberger, and T. De Groeve, 2015. On the Use of Global Flood Forecasts and Satellite-Derived Inundation Maps for Flood Monitoring in Data-Sparse Regions. *Remote Sensing* 7(11):15702-15728. <https://doi.org/10.3390/rs71115702>.
- Schumann, G., G. Di Baldassarre, D. Alsdorf, and P.D. Bates, 2010. Near Real-Time Flood Wave Approximation on Large Rivers from Space: Application to the River Po, Italy. *Water Resources Research* 46(5):W05601, <https://doi.org/10.1029/2008WR007672>.
- USACE (United States Army Corps of Engineers), 2017. Hydrologic Engineering, Center. <http://www.hec.usace.army.mil/software/hec-ras/>.
- USGS (U.S. Geological Survey), 2017. Flood Information. <https://water.usgs.gov/floods/FEV/>.
- Xu, F.G., X.G. Yang, and J.W. Zhou, 2016. Dam-Break Flood Risk Assessment and Mitigation Measures for the Hongshiyuan Landslide-Dammed Lake Triggered by the 2014 Ludian Earthquake. *Geomatics, Natural Hazards and Risk* 1-19, <https://doi.org/10.1080/19475705.2016.1269839>.